Experimental Densities and Calculated Fractional Free Volumes of Ionic Liquids with Tri- and Tetra-substituted Imidazolium Cations

Shuwen Yue, John D. Roveda, Max S. Mittenthal, Matthew S. Shannon & Jason E. Bara*

Department of Chemical & Biological Engineering, University of Alabama, Tuscaloosa, AL USA 35487-0203

*Corresponding author's email address: jbara@eng.ua.edu Fax: +1 205-348-7558

Email addresses for all authors: S. Yue (syue1@crimson.ua.edu); J. D. Roveda (jdroveda@crimson.ua.edu); M. S. Mittenthal (mmitthental@crimson.ua.edu); M. S. Shannon (mlshannon@crimson.ua.edu); J. E. Bara (jbara@eng.ua.edu)

ABSTRACT

Although it has been estimated that there are at least 1 million ionic liquids (ILs) that are accessible using commercially available starting materials, a great portion of the ILs that have been experimentally synthesized, characterized and studied in a variety of applications are built around the relatively simple 1-*n*-alkyl-3-methylimidazolium ([$C_n$mim]) cation motif. Yet, there is no fundamental limitation or reason as to why tri- or tetra-functionalized imidazolium cations have received far less attention. Scant physical property data exist for just a few tri-functionalized imidazolium-based ILs and there is virtually no data on tetra-functionalized ILs. Thus, there are a broad experimental spaces on the "map" of ILs that are largely unexplored. We have sought to make an initial expedition into these "uncharted waters" and have synthesized imidazolium-based ILs with one more functional group(s) at the C(2), C(4) and/or C(5) positions of the imidazolium ring (as well as N(1) and N(3)). This manuscript reports the synthesis and experimental densities of these tri- and tetra-functionalized ILs as well as calculated densities and fractional free volumes from COSMOTherm. To the best of our knowledge, this is the first report of any detailed experimental measurements or computational studies relating to ILs with substitutions at the C(4) and C(5) positions.

1. INTRODUCTION

It has been hypothesized that there are at least 1 million ionic liquids that can be synthesized using readily available starting materials.[1] Yet, despite this broad space, there has been a relatively narrow focus on ILs comprising 1-*R*-3-methylimidazolium cations ($[Rmim]^+$) with various anions ($[X]^-$), or [Rmim][X] ILs (Figure 1).

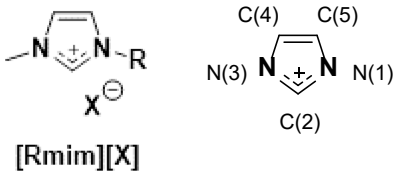

[Rmim][X]

Figure 1: General structure of [Rmim][X] ILs (left) and numerical assignment of positions within the 5-membered imidazole/imidazolium ring starting with N(1) and moving clockwise to C(5) (right).

Generally, [Rmim][X] ILs are produced via quaternization of 1-methylimidazole with a corresponding organohalide (R-X, X = Cl, Br or I), often followed by anion-exchange to molecular anions such as tetrafluoroborate (BF_4^-), hexafluorophosphate (PF_6^-), triflate (OTf^-), bistriflimide (Tf_2N^-) and others. In addition to ubiquitous *n*-alkyl substituents, imidazolium cations a variety of other 'R' groups have been synthesized including: branched and cycloalkyl,[2] hydroxyl-terminated alkyl,[3, 4] nitrile-terminated alkyl,[5, 6] oligo(ethylene glycol) (i.e., ether),[3, 5-8] fluoroalkyl,[9-11] benzyl,[12, 13] silane[12, 14] and siloxane.[14]

It is well-established that both the type of anion and the nature/length of the 'R' group have strong influence over the thermophysical properties of [Rmim][X] ILs,[15-17] and for this reason ILs are considered "designer" solvents. Group contribution methods have been put forth to rapidly and accurately predict properties such as density solely from the IL structure.[18, 19]

Over the past 15+ years, [Rmim][X] ILs have received significant interest as physical solvents for CO_2 absorption,[20-23] and this topic has been extensively studied from experimental, thermodynamic and computational approaches.[24-28] Our research group has proposed that the solubility of CO_2 and other gases in systematically varied [Rmim][X] ILs may be explained by fractional free volume (FFV) (i.e., the portion of empty space within a liquid or solid). While models have been put forth in an effort to relate IL molar volume (i.e., the size of the cation-anion pair) to CO_2 solubility, we postulated that the free volume within ILs may be the more appropriate property by which to understand CO_2 solubility in [Rmim][X] ILs, as it is within this free volume that gases will dissolve. Given the relatively strong Coulombic interactions between cations and anions, the free volume in ILs may be largely due to the weak interactions between the non-polar alkyl 'R' groups. For example, when 'R' is an *n*-alkyl chain (e.g. butyl) extending the length of the chain (e.g. octyl) increases FFV but decreases the solubility of CO_2 in the IL on the basis of mol CO_2/kg IL or mol CO_2/m^3 IL. The solubility of CO_2 would appear to increase on a mole fraction (Henry's Constant) basis, but this is due to the increasing MW of the IL. The increase in FFV is offset by the increasing non-polar character of the IL 'R' group which begins to disfavor additional CO_2 dissolution at given T, P conditions. ILs with smaller FFV were also observed to exhibit higher

selectivity for CO_2 relative to N_2 or CH_4, as the cavity sizes would exclude more of the larger N_2 and CH_4 molecules .[6, 29]

In the [Rmim][X] ILs where 'R' is alkyl, the anion tends to associate with the "acidic" proton bound to the carbon between the two nitrogen atoms in the imidazolium ring (cf. Figure 1).[30-32] However, when 'R' is capable of acting as a H-bond acceptor, such as for oligo(ethylene glycol) substituents, the ether oxygen atom(s) may compete with the anion to H-bond with the C(2)-H proton,[7] resulting in an increase in density and decrease in FFV.[5, 6] For ILs where R was varying lengths of fluoroalkyl groups, the large electron withdrawing effect of the fluorine atoms makes the imidazolium C(2)-H a stronger H-bond donor resulting in increased interactions with the anion.[9, 10]

Thus, it should be of fundamental interest to the study of IL properties as to how density and FFV are affected when the ability of the anion to H-bond with the imidazolium C(2)-H proton is reduced or completely blocked. This can be accomplished through the introduction of one or more electron donating groups (e.g., Me, Et) at the C(2), C(4) and/or C(5) positions. While [Rmim][X] ILs dominate the literature, the functionalization of the imidazole/imidazolium ring is by no means limited to the N(1) and N(3) positions.[33] Tri-, tetra- and even penta-functionalized ILs are accessible through the corresponding imidazole precursors.[31] In fact, 1,2-dimethylimidazole is commercially available in bulk quantities similar to 1-methylimidazole, although 1,2,3-trifunctionalized imidazolium-based ILs are far less prevalent in the literature than 1,3-disubstituted imidazolium-based ILs. 1,2,3-trifunctionalized imidazolium-based ILs are reported to be more thermally and chemically stable than their 1,3-difunctionalized counterparts.[34, 35]

A SciFinder® structure search performed in preparation of this manuscript during October 2017 found that 1-ethyl-2,3-dimethylimidazolium bistriflimide ($[C_2C_1{}^{(2)}mim][Tf_2N]$) had only 116 literature references (excluding patents) while 1-ethyl-3-methylimidazolium bistriflimide ($[C_2mim][Tf_2N]$) had 2621 references (excluding patents). Furthermore, 1-ethyl-3,4(5)-dimethylimidazolium bistriflimide ($[C_2C_1{}^{(4)}mim][Tf_2N]$) has but a single literature reference in Bonhote, et al.,[36] which is one of the earliest and most cited papers on imidazolium-based ILs.

Strangely, despite the interest in a 1,3,4(5)-trisubstituted imidazolium-based IL at the onset of the modern era of IL research in the late 1990s, there has been little to no interest in further studies on this configuration of the imidazolium cation or 1,2,3,4(5)-tetrasubstituted imidazolium-based ILs save for reports from Hayashi, et al.[37] and Gabric, et al.[38] For whatever reason this trend has persisted in the IL research community, it is not due to limitations on the availability of the proper imidazole-based starting materials. A number of imidazoles substituted at the C(2), C(4) and/or C(5) positions are available through specialty chemical suppliers or can be prepared in useful quantities in the laboratory via the Debus-Radziszewksi synthesis.[39-44] Previously, we reported on a facile synthetic method for 1,2-dialkyl, 1,4(5)-dialkyl and 1,2,4(5)-trialkylimidazoles,[45] which are the requisite precursors for accessing tri- and tetra-substituted imidazolium-based ILs. It should be noted that 1,4- and 1,5-dialkylimidazoles (as well as 1,2,4- and 1,2,5-trialkylimidazoles) are synthesized as a mixture of isomers from 4-methylimidazole (or 2-ethyl-4-methylimidazole) and these isomers are extremely difficult to separate. For this reason, the '4(5)' notation is used to describe these compounds.

Perhaps even rarer are 1,3,4,5-tetrasubstituted imidazolium salts,[46, 47] for which the requisite 1,4,5-trimethylimidazole (or similar) starting material has typically not been readily available. However,

a new synthetic method published by Evjen and Fiksdahl may open new opportunities for investigations into 1,3,4,5-tetramethylimidazolium ILs.[39]

Given that that certain tri- and tetra-substituted ILs are readily produced in the laboratory from di- and tri-functionalized imidazoles, it should be of fundamental interest to the study of ILs as to how the distribution of functionalities on the imidazole/imidazolium ring affects properties such as IL density and FFV. Ludwig and co-workers have studied the importance of H-bonds and "H-bond defects" on IL physical properties and structures using a set of eight ILs wherein the five positions of the imidazole ring were substituted with either –H or $–CH_3$ groups.[30-32, 48] Several reports have published density data over a limited temperature range for 1-*n*-alkyl-2,3-dimethylimidazolium salts with $[Tf_2N]^-$, $[BF_4]^-$ and $[PF_6]^-$ anions.[49-53]

Herein, we present experimental density data over the temperature range of (293.15 – 373.15) K for three series of ILs (Figure 2). For ILs which are constitutional isomers (i.e., same chemical formula and molecular weight (MW)), comparative plots of density relative to temperature are presented along with published densities for $[Rmim][Tf_2N]$ IL constitutional isomers. Furthermore, the experimental density data have been compared using values calculated at 298.15 K using COSMOTherm. FFV values for all of the IL series shown in Figure 2 were also calculated using COSMOTherm and an analysis of FFV of constitutional isomers is presented.

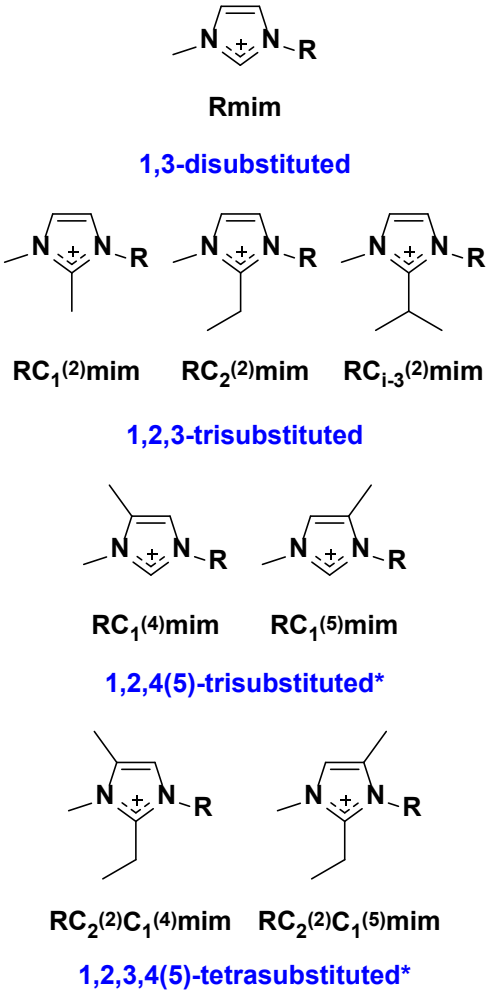

Figure 2: Structures of imidazolium cations considered in this work. Species marked with * denote that these compounds occur together as mixtures of isomers.

2. EXPERIMENTAL

2.1 Materials

The source and purity of all starting materials, solvents reagents and IL products are listed in Table 1. With the exception of 1,2-dimethylimidazole, all other imidazoles were synthesized in our prior study.[45] A table showing the molecular structure of each individual imidazolium cation and the $[Tf_2N]^-$ anion is provided as Supporting Information (Table S1). The IUPAC name and CAS registry number (where available) for each IL is also provided as Supporting Information (Table S2).

Table 1: Source and purity for all starting materials, solvents, reagents and IL products.

Chemical Name	Source	Purification Method	Final Mass Fraction Purity
1,2-dimethylimidazole	Alfa Aesar	No further purification	> 0.980
bromoethane	Alfa Aesar	No further purification	> 0.980
1-bromopropane	Alfa Aesar	No further purification	> 0.990
1-bromobutane	Alfa Aesar	No further purification	> 0.980
1-bromohexane	Alfa Aesar	No further purification	> 0.990
iodomethane	Alfa Aesar	No further purification	> 0.990
lithium bistriflimide	IoLiTec	No further purification	> 0.980
silver nitrate	Alfa Aesar	No further purification	> 0.999
magnesium sulfate	JT Baker	No further purification	> 0.998
acetonitrile	BDH	No further purification	> 0.995
diethyl ether	BDH	No further purification	> 0.980
dichloromethane	BDH	No further purification	> 0.995
1-ethyl-4(5)-methylimidazole*	Our prior work	No further purification	> 0.990
1-propyl-4(5)-methylimidazole*	Our prior work	No further purification	> 0.990
1-butyl-4(5)-methylimidazole*	Our prior work	No further purification	> 0.990
1-hexyl-4(5)-methylimidazole*	Our prior work	No further purification	> 0.990
1,2-diethyl-4(5)-methylimidazole*	Our prior work	No further purification	> 0.990
1-propyl-2-ethyl-4(5)-methylimidazole*	Our prior work	No further purification	> 0.990
1-butyl-2-ethyl-4(5)-methylimidazole*	Our prior work	No further purification	> 0.990
1-hexyl-2-ethyl-4(5)-methylimidazole*	Our prior work	No further purification	> 0.990
$[C_2C_1^{(2)}mim][Tf_2N]$	Synthesis	Vacuum drying	> 0.990
$[C_3C_1^{(2)}mim][Tf_2N]$	Synthesis	Vacuum drying	> 0.990
$[C_4C_1^{(2)}mim][Tf_2N]$	Synthesis	Vacuum drying	> 0.990
$[C_6C_1^{(2)}mim][Tf_2N]$	Synthesis	Vacuum drying	> 0.990
$[C_2C_1^{(4/5)}mim][Tf_2N]$*	Synthesis	Vacuum drying	> 0.990
$[C_3C_1^{(4/5)}mim][Tf_2N]$*	Synthesis	Vacuum drying	> 0.990
$[C_4C_1^{(4/5)}mim][Tf_2N]$*	Synthesis	Vacuum drying	> 0.990
$[C_6C_1^{(4/5)}mim][Tf_2N]$*	Synthesis	Vacuum drying	> 0.990
$[C_2C_2^{(2)}C_1^{(4/5)}mim][Tf_2N]$*	Synthesis	Vacuum drying	> 0.990
$[C_3C_2^{(2)}C_1^{(4/5)}mim][Tf_2N]$*	Synthesis	Vacuum drying	> 0.990
$[C_4C_2^{(2)}C_1^{(4/5)}mim][Tf_2N]$*	Synthesis	Vacuum drying	> 0.990
$[C_6C_2^{(2)}C_1^{(4/5)}mim][Tf_2N]$*	Synthesis	Vacuum drying	> 0.990

*exists as mixture of 4-methyl and 5-methyl isomers (see synthesis section for relative % of each isomer as reported in our prior work). The molar ratios of 4-methyl to 5-methyl isomers initially present in the imidazole starting material are the same in the IL product.

2.2 IL Synthesis

Synthetic methods followed previously published procedures reported for the synthesis of [Rmim][Tf_2N] ILs.[4, 5] ^{1}H NMR spectra are provided as Supporting Information (Figures S1-S12) and indicate all ILs were of at least 0.99 mass fraction purity. IL water content was determined using a Karl-Fisher titration (Mettler Toledo C20) with all having < 3 x 10^{-4} mass fraction residual water after vacuum drying. All ILs were tested using silver nitrate ($AgNO_3$) to confirm the absence of residual halide ions.

1,2,3-trialkylimidazolium ILs (**1-4**) were produced via alkylation of 1,2-dimethylimidazole with a series of 1-bromoalkanes and subsequent ion exchange with lithium bistriflimide ($LiTf_2N$) according to Scheme 1.

Scheme 1: General synthetic scheme for 1-R-2,3-trifunctionalized imidazolium bistriflimide ILs (**1-4**).

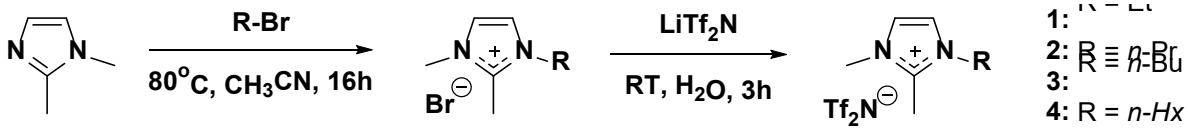

1,3,4-trialkylimidazolium ILs (**5-8**) and 1,2,3,4(5)-tetraalkylimidazolium ILs (**9-12**) were produced via reaction of di- and tri-substituted imidazole compounds with iodomethane followed by ion exchange with $LiTf_2N$ according to Scheme 2.

Scheme 2: General synthetic scheme for 1-R-3,4(5)-trifunctionalized and 1-R-2,3,4(5)-tetrafunctionalized imidazolium bistriflimide ILs (**5-12**).

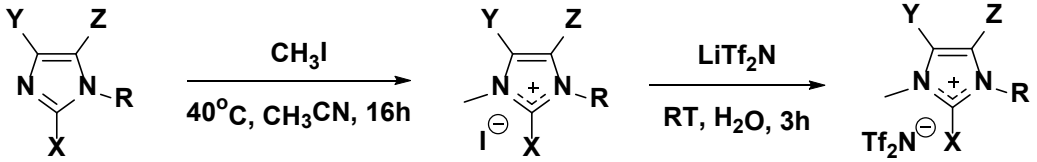

5: R = Et, X = H, Y = H or Me, Z= H or Me
6: R ≡ *n*-Pr, X = H, Y = H or Me, Z= H or Me
7: R = *n*-Bu, X = H, Y = H or Me, Z= H or Me
8: R = *n-Hx,* X = H, Y = H or Me, Z= H or Me
9: R = Et, X = Et, Y = H or Me, Z= H or Me
10: R ≡ *n*-Pr, X = Et, Y = H or Me, Z= H or Me
11: R = *n*-Bu, X = Et, Y = H or Me, Z= H or Me
12: R = *n-Hx,* X = Et, Y = H or Me, Z= H or Me

The mass fraction of water in all ILs synthesized was determined using Karl-Fisher titration (Mettler Toledo C20) to be less than 3 x 10^{-4}. ^{1}H NMR spectra of ILs were obtained using Bruker AV-360 and AV-500 instruments.

1-ethyl-2,3-dimethylimidazolium bistriflimide ([$C_2C_1^{(2)}$mim][Tf_2N]). (1) 1,2-dimethylimidazole (9.39 g, 97.68 mmol) was reacted with bromoethane (12.80 g, 117.46 mmol) in CH_3CN (40 mL) at 40 °C for 16 h. The reaction was then poured into 250 mL of Et_2O, and the mixture stored at -10 °C overnight to achieve crystallization of the crude imidazolium bromide salt. Et_2O was then decanted and 100 mL of deionized H_2O was added to dissolve the residual solid. The aqueous solution was then washed with 3x 50 mL

Et_2O. $LiTf_2N$ (30.85 g, 107.46 mmol) was then added to aqueous phase and an oily precipitate was observed to form almost immediately. The mixture was allowed to stir for at least 3 h. After this time, the aqueous layer was then decanted and the oily product was dissolved in 250 mL of CH_2Cl_2. The organic phase was then washed with 5x 75 mL deionized H_2O. After the fifth aqueous wash, a small amount (~5 mg) of $AgNO_3$ was added to the aqueous wash. The absence of a precipitate indicated that residual halide was below detectable levels. The organic phase was then washed with an additional 2x 75 mL deionized H_2O. Anhydrous $MgSO_4$ was then added to the organic phase as a drying agent. The solids were filtered and the product was then concentrated via rotary evaporation and further dried under dynamic vacuum (< 1 mm Hg) while stirring at 40°C overnight to produce **1** as a transparent liquid in 81.0 % yield (32.1 g). ^{1}H NMR (500 MHz, DMSO-d_6) δ 7.65 (d, *J* = 2.1 Hz, 1H), 7.61 (d, *J* = 2.1 Hz, 1H), 4.14 (q, *J* = 7.3 Hz, 2H), 3.74 (s, 3H), 2.58 (s, 3H), 1.34 (t, *J* = 7.3 Hz, 3H).

1-propyl-2,3-dimethylimidazolium bistriflimide ($[C_3C_1^{(2)}mim][Tf_2N]$). (2) 1,2-dimethylimidazole (10.70 g, 111.31 mmol) was reacted with 1-bromopropane (16.50 g, 134.16mmol) followed by ion exchange with $LiTf_2N$ (35.15 g, 122.44 mmol) using the same procedure as (1) in 74.5 % yield (34.8 g). ^{1}H NMR (500 MHz, DMSO-d_6) δ 7.63 (dd, *J* = 13.4, 2.1 Hz, 2H), 4.07 (dd, *J* = 7.7, 6.8 Hz, 2H), 3.75 (s, 3H), 2.58 (s, 3H), 1.73 (h, *J* = 7.4 Hz, 2H), 0.87 (t, *J* = 7.4 Hz, 3H).

1-butyl-2,3-dimethylimidazolium bistriflimide ($[C_4C_1^{(2)}mim][Tf_2N]$). (3) 1,2-dimethylimidazole (6.00 g, 62.42 mmol) was reacted with 1-bromobutane (10.33 g, 75.39 mmol) followed by ion exchange with $LiTf_2N$ (19.71 g, 68.65 mmol) using the same procedure as (1) in 55.5 % yield (15.0 g). ^{1}H NMR (500 MHz, DMSO-d_6) δ 7.62 (dd, *J* = 15.7, 2.1 Hz, 2H), 4.10 (t, *J* = 7.3 Hz, 2H), 3.74 (s, 3H), 2.58 (s, 3H), 1.74 – 1.64 (m, 2H), 1.29 (dq, *J* = 14.8, 7.4 Hz, 2H), 0.91 (t, *J* = 7.4 Hz, 3H).

1-hexyl-2,3-dimethylimidazolium bistriflimide ($[C_6C_1^{(2)}mim][Tf_2N]$). (4) 1,2-dimethylimidazole (6.13g, 63.72 mmol) was reacted with 1-bromohexane (12.60 g, 76.33 mmol) followed by ion exchange with $LiTf_2N$ (20.12 g, 70.08 mmol) using the same procedure as (1) in 62.7% yield (18.4 g). ^{1}H NMR (500 MHz, DMSO-d_6) δ 7.62 (dd, *J* = 18.1, 2.1 Hz, 2H), 4.20 – 3.99 (m, 2H), 3.74 (s, 3H), 2.57 (s, 3H), 1.70 (p, *J* = 7.6 Hz, 2H), 1.27 (q, *J* = 6.2, 4.5 Hz, 6H), 1.04 – 0.77 (m, 3H).

1-ethyl-3,4(5)-dimethylimidazolium bistriflimide ($[C_2C_1^{(4/5)}mim][Tf_2N]$). (5) 1-ethyl-4(5)-methylimidazole (6.02 g, 54.60 mmol, 60.2 % 4-methyl isomer) was reacted with iodomethane (20.0 g, 140.90 mmol) in CH_3CN (40 mL) at 40 °C for 16 h. The reaction was poured into 250 mL of Et_2O, and the mixture stored at -10 °C overnight to achieve crystallization of the crude imidazolium iodide salt. Et_2O was then decanted and 100 mL of deionized H_2O water was added to then dissolve the residual solid. The aqueous solution was then washed with 3x 50 mL Et_2O. $LiTf_2N$ (17.24 g, 60.06 mmol) was then added to the aqueous phase and an oily precipitate was observed to form almost immediately. The mixture was allowed to stir for at least 3 h. After this time, the aqueous layer was carefully decanted, and the oily product was dissolved in 300 mL of CH_2Cl_2. The solution was subsequently washed with 6x 100 mL deionized H_2O. The product was then concentrated via rotary evaporation and further dried under dynamic vacuum (< 1 mm Hg) at 40°C overnight to produce **5** as a transparent liquid in 71.0% yield (15.7 g). ^{1}H NMR (500 MHz, DMSO-d_6) δ 9.01 (s, 1H), 7.65 – 7.35 (m, 1H), 4.27 – 4.01 (m, 2H), 3.76 (dd, *J* = 33.1, 0.6 Hz, 3H), 2.27 (dd, *J* = 12.1, 1.1 Hz, 3H), 1.39 (td, *J* = 7.3, 3.4 Hz, 3H).

1-propyl-3,4(5)-dimethylimidazolium bistriflimide ($[C_3C_1^{(4/5)}mim][Tf_2N]$). (6) 1-propyl-4(5)-methylimidazole (6.05 g, 48.68 mmol, 62.9 % 4-methyl isomer) was reacted with iodomethane (17.36 g, 122.31 mmol) followed by ion exchange with $LiTf_2N$ (15.37 g, 53.54 mmol) using the same procedure as

(5) in 86.1 % yield (17.6 g). ^{1}H NMR (360 MHz, DMSO-d_6) δ 9.02 (d, *J* = 1.8 Hz, 1H), 7.59 – 7.34 (m, 1H), 4.07 (q, *J* = 6.9 Hz, 2H), 3.78 (d, *J* = 23.8 Hz, 3H), 2.28 (dd, *J* = 6.5, 1.1 Hz, 3H), 1.78 (hd, *J* = 7.3, 5.5 Hz, 2H), 0.88 (dt, *J* = 14.9, 7.4 Hz, 3H).

1-butyl-3,4(5)-dimethylimidazolium bistriflimide ([$C_4C_1^{(4/5)}$mim][Tf_2N]). (7) 1-butyl-4(5)-methylimidazole (6.01 g, 43.45 mmol, 63.7 % 4-methyl isomer) was reacted with iodomethane (15.40 g, 108.50 mmol) followed by ion exchange with $LiTf_2N$ (13.73 g, 47.82 mmol) using the same procedure as (5) in 76.7 % yield (14.4 g). ^{1}H NMR (500 MHz, DMSO-d_6) δ 9.06 – 8.90 (m, 1H), 7.51 (dd, *J* = 1.8, 1.1 Hz, 1H), 4.09 (dt, *J* = 12.8, 7.2 Hz, 2H), 3.76 (d, *J* = 33.1 Hz, 3H), 2.27 (dd, *J* = 11.5, 1.1 Hz, 3H), 1.78 – 1.66 (m, 2H), 1.42 – 1.12 (m, 2H), 0.91 (dt, *J* = 10.4, 7.4 Hz, 3H).

1-hexyl-3,4(5)-dimethylimidazolium bistriflimide ([$C_6C_1^{(4/5)}$mim][Tf_2N]). (8) 1-hexyl-4(5)-methylimidazole (6.00 g, 36.11 mmol, 63.7 % 4-methyl isomer) was reacted with iodomethane (12.85 g, 90.53 mmol) followed by ion exchange with $LiTf_2N$ (10.46 g, 36.43 mmol) using the same procedure as (5) in 76.7 % yield (12.8 g). ^{1}H NMR (500 MHz, DMSO-d_6) δ 9.01 (d, *J* = 1.7 Hz, 1H), 7.51 (dt, *J* = 2.2, 1.1 Hz, 1H), 4.09 (t, *J* = 7.2 Hz, 2H), 3.87 – 3.66 (m, 3H), 2.27 (dd, *J* = 9.8, 1.1 Hz, 3H), 1.75 (p, *J* = 7.4 Hz, 2H), 1.38 – 1.14 (m, 6H), 1.02 – 0.73 (m, 3H).

1,2-diethyl-3,4(5)-dimethylimidazolium bistriflimide ([$C_2C_2^{(2)}C_1^{(4/5)}$mim][Tf_2N]). (9) 1,2-diethyl-4(5)-methylimidazole (43.00 g, 311.12 mmol, 73.5 % 4-methyl isomer) was reacted with iodomethane (91.20 g, 642.53 mmol) followed by ion exchange with $LiTf_2N$ (80.80 g, 281.44 mmol) using the same procedure as (5) in 73.6 % yield (99.19 g). ^{1}H NMR (360 MHz, DMSO-d_6) δ 7.41 (d, J = 29.1 Hz, 1H), 4.12 (ddd, J = 12.3, 6.0, 4.0 Hz, 2H), 3.70 (dd, J = 32.3, 2.0 Hz, 3H), 3.17 – 2.85 (m, 2H), 2.26 (dd, J = 12.7, 1.9 Hz, 3H), 1.49 – 0.96 (m, 6H).

1-propyl-2-ethyl-3,4(5)-dimethylimidazolium bistriflimide ([$C_3C_2^{(2)}C_1^{(4/5)}$mim][Tf_2N]). (10) 1-propyl-2-ethyl-4(5)-methylimidazole (6.05g, 39.77 mmol, 76.3 % 4-methyl isomer) was reacted with iodomethane (15.00 g, 105.68 mmol) followed by ion exchange with $LiTf_2N$ (12.57 g, 43.77 mmol) using the same procedure as (5) in 78.0 % yield (13.9 g). ^{1}H NMR (500 MHz, DMSO-d_6) δ 7.44 (q, *J* = 1.1 Hz, 1H), 4.14 – 3.97 (m, 2H), 3.70 (d, *J* = 45.4 Hz, 3H), 3.04 (q, *J* = 7.7 Hz, 2H), 2.26 (dd, *J* = 12.2, 1.1 Hz, 3H), 1.88 – 1.57 (m, 2H), 1.29 – 1.08 (m, 3H), 0.91 (dt, *J* = 21.4, 7.4 Hz, 3H).

1-butyl-2-ethyl-3,4(5)-dimethylimidazolium bistriflimide ([$C_4C_2^{(2)}C_1^{(4/5)}$mim][Tf_2N]). (11) 1-butyl-2-ethyl-4(5)-methylimidazole (6.10 g, 36.71 mmo), 80.6 % 4-methyl isomer) was reacted with iodomethane (13.70 g, 96.52 mmol) followed by ion exchange with $LiTf_2N$ (11.60 g, 40.41 mmol) using the same procedure as (5) in 80.9 % yield (13.7 g). ^{1}H NMR (500 MHz, DMSO-d_6) δ 7.44 (q, *J* = 1.2 Hz, 1H), 4.07 (t, *J* = 7.4 Hz, 2H), 3.70 (d, *J* = 45.9 Hz, 3H), 3.03 (q, *J* = 7.6 Hz, 2H), 2.26 (dd, *J* = 15.0, 1.1 Hz, 3H), 1.81 – 1.53 (m, 2H), 1.31 (ddt, *J* = 22.5, 14.8, 7.4 Hz, 2H), 1.17 (dt, *J* = 9.6, 7.6 Hz, 3H), 0.92 (dt, *J* = 9.1, 7.4 Hz, 3H).

1-hexyl-2-ethyl-3,4(5)-dimethylimidazolium bistriflimide ([$C_6C_2^{(2)}C_1^{(4/5)}$mim][Tf_2N]). (12) 1-hexyl-2-ethyl-4(5)-methylimidazole (7.12 g, 36.65 mmol, 81.3 % 4-methyl isomer) was reacted with iodomethane (13.95 g, 98.29 mmol) followed by ion exchange with $LiTf_2N$ (11.59 g, 40.37 mmol) using the same procedure as (5) in 73.7 % yield (13.2 g). ^{1}H NMR (500 MHz, DMSO-d_6) δ 7.45 (d, *J* = 1.3 Hz, 1H), 4.20 – 3.95 (m, 2H), 3.70 (d, *J* = 45.6 Hz, 3H), 3.03 (q, *J* = 7.6 Hz, 2H), 2.26 (dd, *J* = 13.2, 1.1 Hz, 3H), 1.71 (t, *J* = 7.4 Hz, 2H), 1.40 – 1.22 (m, 6H), 1.17 (dt, *J* = 9.5, 7.6 Hz, 3H), 0.95 – 0.81 (m, 3H).

2.3 Density Measurements

Densities of ILs (**1-12**) were experimentally determined using a Mettler Toledo DM45 DeltaRange oscillating U-tube densitometer over the range of (293.15 – 373.15) K at 101.325 kPa in increments of 10.00 K in the same manner as our prior work.[54] The accuracy of the density meter measurements is 5 x 10^{-5} g.cm^3 at all temperatures. The limit of error in the cell temperature is +/- 0.05 K as controlled by a Peltier element. The calibration of the unit was verified using water standards provided by the manufacturer. The sample cell was cleaned between by flushing the sample from the cell by injecting air, followed by cleaning with acetone and drying the cell by injecting air until the cell reading was verified to be consistent with the density of air at 293.15 K (0.00120 g.cm^{-3}).

3. COMPUTATIONAL METHODS

Density, molar volume and FFV for the $[Tf_2N]^-$ salts of the eight families of tri- and tetra-substituted imidazolium cations depicted in Figure 2 were calculated using the COSMOTherm software package (v. C30_1301, COSMOlogic, Leverkusen, Germany) following methods previously outlined by our group and others.[6, 55-57] This set includes the 20 imidazolium cations present in ILs **1-12** and an additional 16 imidazolium cations from the $[Rmim]^+$, 1-R-2-ethyl-3-methylimidazolium ($[RC_2{}^{(2)}mim]^+$) and 1-R-2-isopropyl-3-methylimidazolium ($[RC_{i\text{-}3}{}^{(2)}mim]^+$) series that were only examined *in silico.* For all series other than $[Rmim][Tf_2N]$, the R groups examined are ethyl, *n*-propyl, *n*-butyl and *n*-hexyl. For $[Rmim][Tf_2N]$ ILs, the R groups examined were ethyl, *n*-propyl, *n*-butyl, *n*-pentyl, *n*-hexyl, *n*-heptyl, *n*-octyl and *n*-nonyl. Cation structures were optimized in TURBOMOLE using the TZVP basis set [58] at the DFT level and using the Becke and Perdew (bp) functional[59,60]. COSMOThermo calculations were also made at the TZVP level. The $[Tf_2N]^-$ anion was available in the COSMOBase library acquired from the software provider. COSMOTherm was used to calculate IL MW ([=] g/mol), IL densities (ρ [=] g/cm^3), molar volumes V_m [=] A^3/mol, and COSMO volumes V_{COSMO} [=] A^3/mol at 298.15 K. From these properties, the dimensionless quantity, fractional free volume (*FFV*), was calculated using Eqn. 1.

$$FFV = \frac{V_m - V_{COSMO}}{V_m} \quad \textbf{(1)}$$

Each $[RC_1{}^{(4)}mim][Tf_2N]$ and $[RC_1{}^{(5)}mim][Tf_2N]$ species are always present as an essentially inseparable mixture. Therefore, densities were predicted in COSMOTherm using the relative amount of each isomer reported in Section 2.2. Similarly, the $[RC_2{}^{(2)}C_1{}^{(4)}mim][Tf_2N]$ and $[RC_2{}^{(2)}C_1{}^{(5)}mim][Tf_2N]$ species were also treated using the isomer ratios reported in Section 2.2. All values calculated by COSMOTherm are available as Supporting Information (Tables S3-S10).

4. RESULTS AND DISCUSSION

Experimentally measured density data for ILs 1-4, 5-8 and 9-12 are presented in Tables 2, 3 and 4, respectively.

Table 2: Densities (ρ) of [$RC_1^{(2)}$mim][Tf_2N] ILs at different temperatures (T) and p = 100.5 kPa with comparisons to literature values where applicable.[a]

$\frac{T}{K}$	$\frac{\rho}{g \cdot cm^{-3}}$		$\frac{T}{K}$	$\frac{\rho}{g \cdot cm^{-3}}$		$\frac{T}{K}$	$\frac{\rho}{g \cdot cm^{-3}}$		$\frac{T}{K}$	$\frac{\rho}{g \cdot cm^{-3}}$	
[$C_2C_1^{(2)}$mim][Tf_2N]			[$C_3C_1^{(2)}$mim][Tf_2N]			[$C_4C_1^{(2)}$mim][Tf_2N]			[$C_6C_1^{(2)}$mim][Tf_2N]		
Exp.		Lit.	Exp.		Lit	Exp.		Lit.	Exp.		Lit.
293.15	1.4964	1.496[52]	293.15	1.4600	1.459[52]	293.15	1.4240	1.424[52] 1.420[50] 1.4240[53]	293.15	1.3622	1.3582[51]
303.15	1.4867	1.487[52]	303.15	1.4503	1.450[52]	303.15	1.4146	1.415[52] 1.4119[50] 1.4148[53]	303.15	1.3531	1.3487[51]
313.15	1.4769	1.477[52]	313.15	1.4407	1.440[52]	313.15	1.4053	1.405[52] 1.4055[53]	313.15	1.3441	1.3399[51]
323.15	1.4673	1.468[52]	323.15	1.4312	1.431[52]	323.15	1.3960	1.396[52] 1.3964[53]	323.15	1.3352	1.3311[51]
333.15	1.4577		333.15	1.4217		333.15	1.3869	1.3873[53]	333.15	1.3263	1.3222[51]
343.15	1.4482		343.15	1.4124		343.15	1.3778	1.3784[53]	343.15	1.3175	
353.15	1.4388		353.15	1.4030		353.15	1.3687	1.3693[53]	353.15	1.3087	

a: standard uncertainties u are $u(T)$ = 0.01 K, u(p) = 0.5 kPa and $u(\rho)$ = 0.001 g.cm^{-3}.

Table 3: Densities of [$RC_1^{(4/5)}$mim][Tf_2N] ILs at different temperatures and p = 100.5 kPa. [a]

$\frac{T}{K}$	$\frac{\rho}{g \cdot cm^{-3}}$	$\frac{T}{K}$	$\frac{\rho}{g \cdot cm^{-3}}$	$\frac{T}{K}$	$\frac{\rho}{g \cdot cm^{-3}}$	$\frac{T}{K}$	$\frac{\rho}{g \cdot cm^{-3}}$
[$C_2C_1^{(4/5)}$mim][Tf_2N] *60.2 % 4-Me Isomer*		[$C_3C_1^{(4/5)}$mim][Tf_2N] *62.9 % 4-Me Isomer*		[$C_4C_1^{(4/5)}$mim][Tf_2N] *63.7 % 4-Me Isomer*		[$C_6C_1^{(4/5)}$mim][Tf_2N] *63.7 % 4-Me Isomer*	
293.15	1.4832	293.15	1.4454	293.15	Solid	293.15	1.3525
303.15	1.4733	303.15	1.4356	303.15	Solid	303.15	1.3433
313.15	1.4634	313.15	1.4259	313.15	1.3911	313.15	1.3342
323.15	1.4536	323.15	1.4163	323.15	1.3810	323.15	1.3252
333.15	1.4439	333.15	1.4069	333.15	1.3723	333.15	1.3163
343.15	1.4342	343.15	1.3973	343.15	1.3631	343.15	1.3074
353.15	1.4246	353.15	1.3879	353.15	1.3539	353.15	1.2985

a: standard uncertainties u are $u(T)$ = 0.01 K, u(p) = 0.5 kPa, $u(x) = 0.01x$ and $u(\rho)$ = 0.001 g.cm^{-3}.

Table 4: Densities of $[RC_2{}^{(2)}{}_1{}^{(4/5)}mim][Tf_2N]$ ILs at different temperatures and p = 100.5 kPa. [a]

$\frac{T}{K}$	$\frac{\rho}{g \cdot cm^{-3}}$	$\frac{T}{K}$	$\frac{\rho}{g \cdot cm^{-3}}$	$\frac{T}{K}$	$\frac{\rho}{g \cdot cm^{-3}}$	$\frac{T}{K}$	$\frac{\rho}{g \cdot cm^{-3}}$
$[C_2C_2{}^{(2)}C_1{}^{(4/5)}mim][Tf_2N]$ *73.5 % 4-Me Isomer*		$[C_3C_2{}^{(2)}C_1{}^{(4/5)}mim][Tf_2N]$ *76.3 % 4-Me Isomer*		$[C_4C_2{}^{(2)}C_1{}^{(4/5)}mim][Tf_2N]$ *80.6 % 4-Me Isomer*		$[C_6C_2{}^{(2)}C_1{}^{(4/5)}mim][Tf_2N]$ *81.3 % 4-Me Isomer*	
293.15	1.4317	293.15	1.4012	293.15	1.3712	293.15	1.3252
303.15	1.4220	303.15	1.3917	303.15	1.3619	303.15	1.3162
313.15	1.4126	313.15	1.3823	313.15	1.3528	313.15	1.3073
323.15	1.4031	323.15	1.3730	323.15	1.3437	323.15	1.2985
333.15	1.3938	333.15	1.3638	333.15	1.3347	333.15	1.2897
343.15	1.3846	343.15	1.3547	343.15	1.3258	343.15	1.2810
353.15	1.3753	353.15	1.3455	353.15	1.3169	353.15	1.2723

a: standard uncertainties u are $u(T)$ = 0.01 K, u(p) = 0.5 kPa, $u(x) = 0.01x$ and $u(\rho)$ = 0.001 g.cm^{-3}.

Tables 2-4 show that for each IL, density decreases with increasing temperature. It can also be observed that for a given cation type (e.g., $[RC_1{}^{(4/5)}mim]$) at a given temperature, the IL density decreases with increasing length of 'R'.

$[RC_1{}^{(2)}mim][Tf_2N]$ ILs are the only ones in this study for which prior experimental data have been reported (Table 2). For all conditions where data have been reported in the literature, the agreement is generally excellent, with differences no greater than 0.004 g.cm^{-3} observed.

Table 5 summarizes the parameters for the density-temperature equation, ρ = -aT +b, for each IL measured.

Table 5: Density-temperature equation parameters for ILs 1-12 (ρ = -aT + b) over temperature range 293.15 – 373.15 K.

IL	Cation	$\frac{a}{10^{-4} \cdot g \cdot cm^{-3} \cdot K}$	$\frac{b}{g \cdot cm^{-3}}$	R^2
1	$[C_2C_1{}^{(2)}mim]$	9.599	1.778	1.0000
2	$[C_3C_1{}^{(2)}mim]$	9.484	1.738	1.0000
3	$[C_4C_1{}^{(2)}mim]$	9.219	1.694	1.0000
4	$[C_6C_1{}^{(2)}mim]$	8.901	1.623	1.0000
5	$[C_2C_1{}^{(4/5)}mim]$	9.774	1.770	1.0000
6	$[C_3C_1{}^{(4/5)}mim]$	9.587	1.726	0.9999
7*	$[C_4C_1{}^{(4/5)}mim]$	9.236	1.680	0.9995
8	$[C_5C_1{}^{(4/5)}mim]$	8.996	1.616	1.0000
9	$[C_2C_2{}^{(2)}C_1{}^{(4/5)}mim]$	9.381	1.706	0.9999
10	$[C_3C_2{}^{(2)}C_1{}^{(4/5)}mim]$	9.270	1.673	0.9999
11	$[C_4C_2{}^{(2)}C_1{}^{(4/5)}mim]$	9.036	1.636	0.9999
12	$[C_6C_2{}^{(2)}C_1{}^{(4/5)}mim]$	8.798	1.583	1.0000

*equation parameters for $[C_4C_1{}^{(4/5)}mim][Tf_2N]$ are valid only from 313.15 K to 373.15 K.

It is expected that the density of a given IL series (e.g., $[RC_1^{(4/5)}mim][Tf_2N]$) can be accurately modeled as a function of both temperature and some parameterization relating to length of R (*n*-alkyl chain) (i.e., ρ = f (T, R)), as has been shown across a series of 1-*n*-alkylimidazoles ranging from 1-methylimidazole to 1-*n*-tetradecylimidazole.[54]

Table 6 presents ILs from this study which are constitutional isomers along with the corresponding $[Rmim][Tf_2N]$ IL.

Table 6: Groups of constitutional isomers among $[Rmim][Tf_2N]$ ILs and ILs prepared in this study.

$\frac{MW}{g \cdot mol^{-1}}$	**$[Rmim][Tf_2N]$**	**$[RC_1^{(2)}mim][Tf_2N]$**	**$[RC_1^{(4/5)}mim][Tf_2N]$**	**$[RC_2^{(2)}C_1^{(4/5)}mim][Tf_2N]$**
405.33	$[C_3mim]$	$[C_2C_1^{(2)}mim]$	$[C_2C_1^{(4/5)}mim]$	N/A
419.36	$[C_4mim]$	$[C_3C_1^{(2)}mim]$	$[C_3C_1^{(4/5)}mim]$	$[C_1C_2^{(2)}C_1^{(4/5)}mim]$*
433.38	$[C_5mim]$	$[C_4C_1^{(2)}mim]$	$[C_4C_1^{(4/5)}mim]$	$[C_2C_2^{(2)}C_1^{(4/5)}mim]$
447.41	$[C_6mim]$	$[C_5C_1^{(2)}mim]$#	$[C_5C_1^{(4/5)}mim]$*	$[C_3C_2^{(2)}C_1^{(4/5)}mim]$
461.44	$[C_7mim]$	$[C_6C_1^{(2)}mim]$	$[C_6C_1^{(4/5)}mim]$	$[C_4C_2^{(2)}C_1^{(4/5)}mim]$
489.49	$[C_9mim]$	$[C_8C_1^{(2)}mim]$#	$[C_8C_1^{(4/5)}mim]$*	$[C_6C_2^{(2)}C_1^{(4/5)}mim]$

'N/A' = this IL is infeasible.

* = These ILs are feasible but were not synthesized here nor have been reported in the literature.

= These ILs have been reported in the literature, although no density data are found in the NIST IL Thermo database.[61]

Table 6 shows that there are 6 groupings of ILs for which experimental density data from this work can be compared against published density data for $[Rmim][Tf_2N]$ ILs from Widegren and Magee ($[C_6mim][Tf_2N]$)[62] and Rocha, et al. (all other $[Rmim][Tf_2N]$).[63] These comparisons are plotted in Figures 3-8.

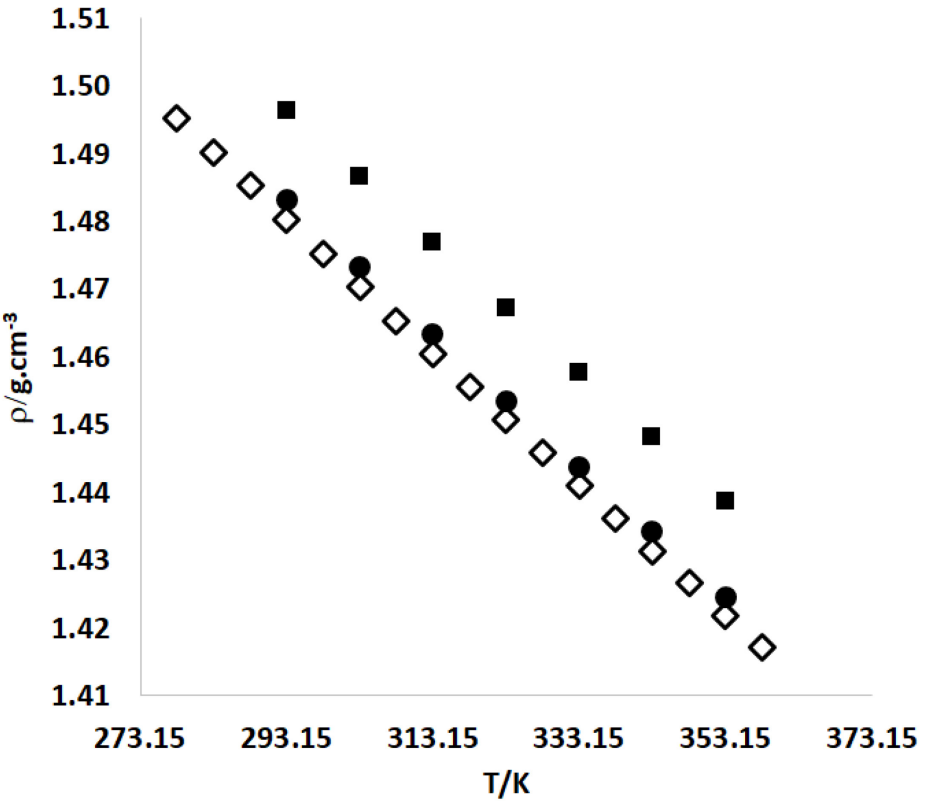

Figure 3: Comparison of density relative to temperature for ILs with MW = 405.33 g.mol^{-1}. ◇ = [C_3mim][Tf_2N]; ● = [$C_2C_1^{(2)}$mim][Tf_2N]; ■ = [$C_2C_1^{(4/5)}$mim][Tf_2N].

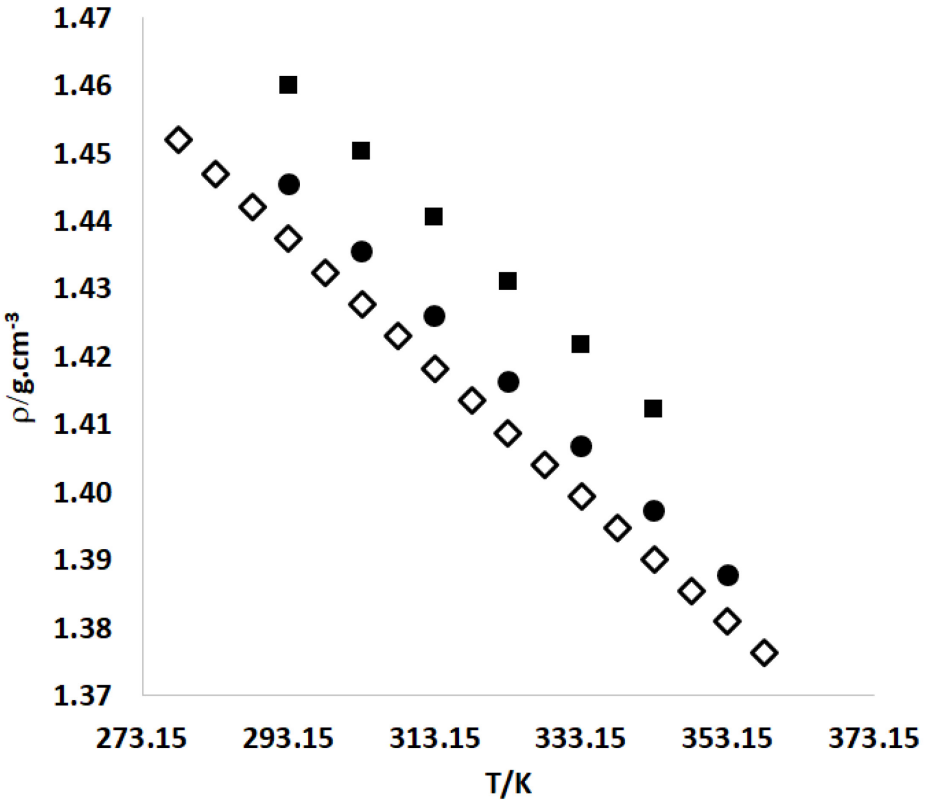

Figure 4: Comparison of density relative to temperature for ILs with MW = 419.36 g.mol^{-1}. ◇ = [C_4mim][Tf_2N]; ● = [$C_3C_1^{(2)}$mim][Tf_2N]; ■ = [$C_3C_1^{(4/5)}$mim][Tf_2N].

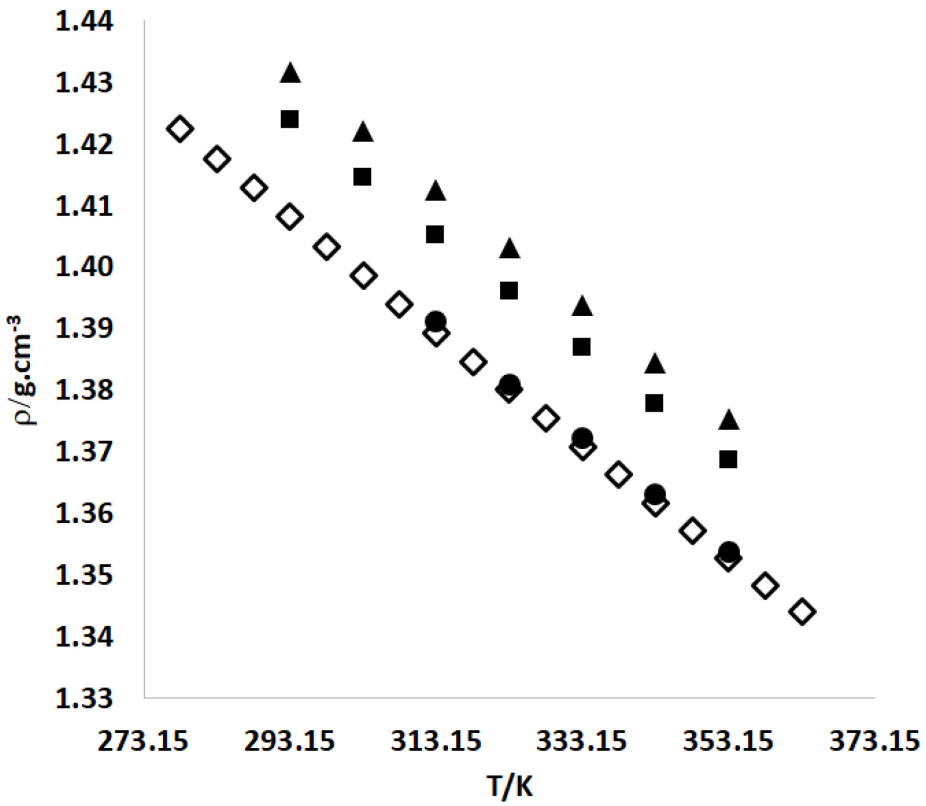

Figure 5: Comparison of density relative to temperature for ILs with MW = 433.38 g.mol^{-1}. ◇= [C_5mim][Tf_2N]; ● = [$C_4C_1^{(2)}$mim][Tf_2N]; ■ = [$C_4C_1^{(4/5)}$mim][Tf_2N]; ▲ = [$C_2C_2^{(2)}C_1^{(4/5)}$mim][Tf_2N].

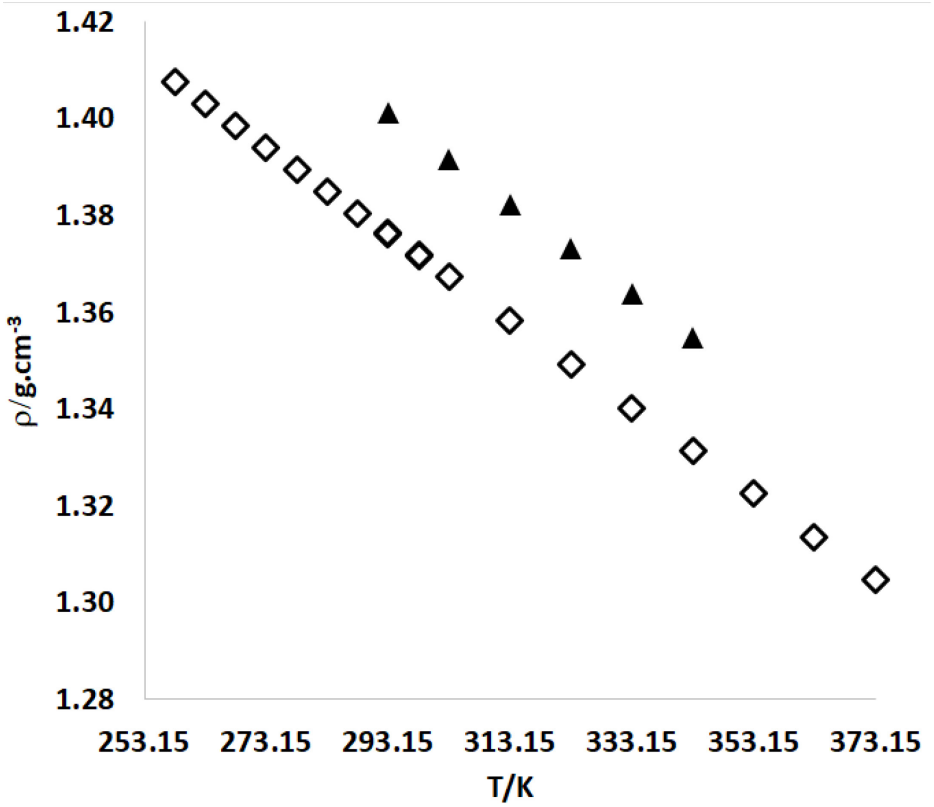

Figure 6: Comparison of density relative to temperature for ILs with MW = 447.41 g.mol^{-1}. ◇= [C_6mim][Tf_2N]; ▲= [$C_3C_2^{(2)}C_1^{(4/5)}$mim][Tf_2N].

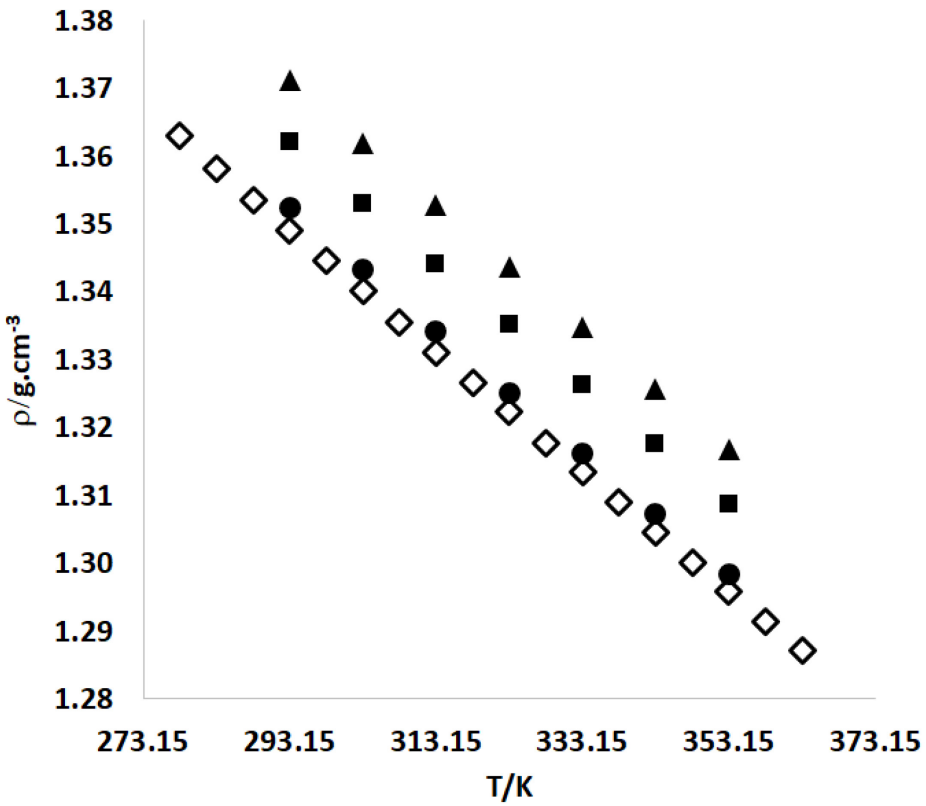

Figure 7: Comparison of density relative to temperature for ILs with MW = 461.44 g.mol^{-1}. ◇ = [C_7mim][Tf_2N]; ● = [$C_6C_1^{(2)}$mim][Tf_2N]; ■ = [$C_6C_1^{(4/5)}$mim][Tf_2N]; ▲= [$C_4C_2^{(2)}C_1^{(4/5)}$mim][Tf_2N].

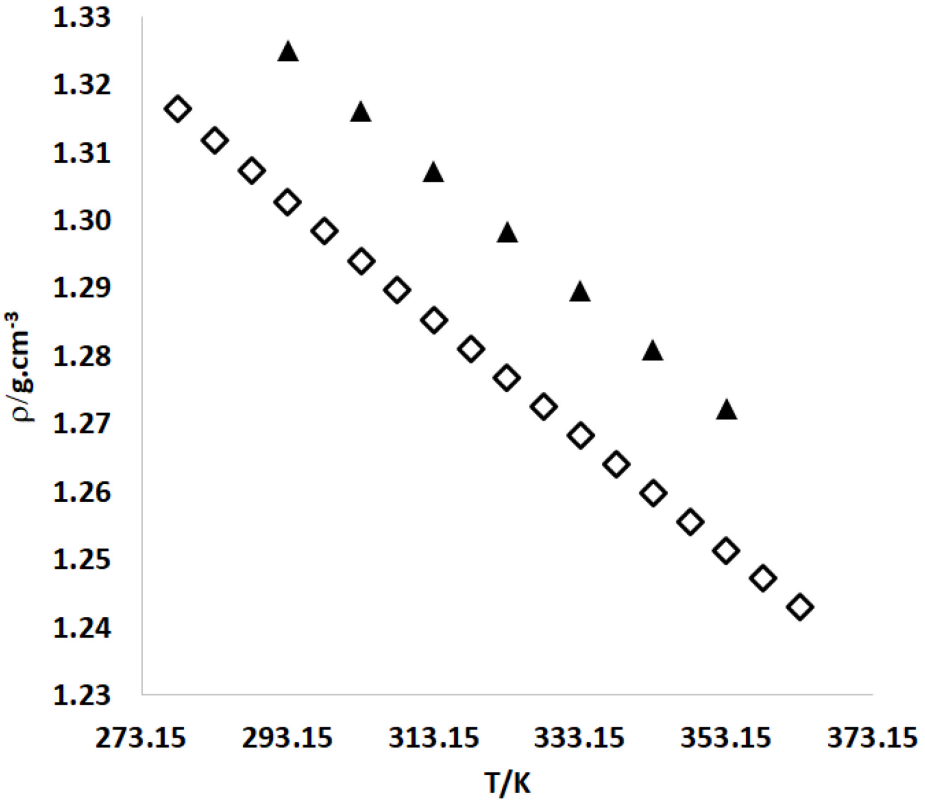

Figure 8: Comparison of density relative to temperature for ILs with MW = 489.49 g.mol^{-1}. ◇= [C_9mim][Tf_2N]; ▲= [$C_6C_2^{(2)}C_1^{(4/5)}$mim][Tf_2N].

Figures 3-8 reveal that for a given MW, the [$RC_2^{(2)}C_1^{(4/5)}$mim][Tf_2N] and [Rmim][Tf_2N] ILs are the most and least dense ILs, respectively. [$RC_1^{(4/5)}$mim][Tf_2N] ILs are only slightly more dense than the [Rmim][Tf_2N] ILs at a given MW, while [$RC_1^{(2)}$mim][Tf_2N] ILs are more dense than these, but less dense than [$RC_2^{(2)}C_1^{(4/5)}$mim][Tf_2N] IL isomers.

In order to understand the influence of the position of the methyl group at the 4- or 5-position in [$RC_1^{(4/5)}$mim][Tf_2N] and [$RC_2^{(2)}C_1^{(4/5)}$mim][Tf_2N] ILs, COSMOTherm was utilized to calculate densities for each of the 16 distinct ILs, where only the pure 4-methyl or 5-methyl isomer is present. The calculated densities for these ILs at 298.15 K are presented in Table 7.

Table 7: Densities (ρ) of [$RC_1^{(4)}$mim][Tf_2N], [$RC_1^{(5)}$mim][Tf_2N], [$RC_2^{(2)}C_1^{(4)}$mim][Tf_2N] and [$RC_2^{(2)}C_1^{(5)}$mim][Tf_2N] ILs at 298.15 K calculated by COSMOTherm.

Cation	$\frac{\rho}{g \cdot cm^{-3}}$	Cation	$\frac{\rho}{g \cdot cm^{-3}}$	Cation	$\frac{\rho}{g \cdot cm^{-3}}$	Cation	$\frac{\rho}{g \cdot cm^{-3}}$
[$C_2C_1^{(4)}$mim]	1.4809	[$C_2C_1^{(5)}$mim]	1.4852	[$C_2C_2^{(2)}C_1^{(4)}$mim]	1.4168	[$C_2C_2^{(2)}C_1^{(5)}$mim]	1.4199
[$C_3C_1^{(4)}$mim]	1.4427	[$C_3C_1^{(5)}$mim]	1.4520	[$C_3C_2^{(2)}C_1^{(4)}$mim]	1.3788	[$C_3C_2^{(2)}C_1^{(5)}$mim]	1.3884
[$C_4C_1^{(4)}$mim]	1.4097	[$C_4C_1^{(5)}$mim]	1.4179	[$C_4C_2^{(2)}C_1^{(4)}$mim]	1.3622	[$C_4C_2^{(2)}C_1^{(5)}$mim]	1.3710
[$C_6C_1^{(4)}$mim]	1.3520	[$C_6C_1^{(5)}$mim]	1.3583	[$C_6C_2^{(2)}C_1^{(4)}$mim]	1.3138	[$C_6C_2^{(2)}C_1^{(5)}$mim]	1.3200

For all of the entries in Table 7, COSMOTherm calculates that the 5-methyl isomer is denser than the 4-methyl isomer by ~0.50-0.75 %. Based on a simple examination of molecular structure, the location of the methyl group at the C(5) position is directly adjacent to N(1), where the larger alkyl chain is present. This configuration may present a slightly more "compact" cation by localizing the alkyl groups to adjacent sites: C(5), N(1) as well as C(2) for $[RC_2^{(2)}C_1^{(5)}mim][Tf_2N]$ ILs. Using the isomer abundances listed in Tables 2 and 3, a simple mole fraction weighted average (Eqn. 2) was used to calculate COSMOTherm-predicted densities for $[RC_1^{(4/5)}mim][Tf_2N]$ and $[RC_2^{(2)}C_1^{(4/5)}mim][Tf_2N]$ ILs at 298.15 K based on their experimentally determined isomer abundances, where $\rho_{COSMO,4\text{-}Me}$ and $\rho_{COSMO,5\text{-}Me}$ are the values in Table 5 for each pair of isomers, and $x_{4\text{-}Me}$ is the mole fraction of the 4-methyl isomer in the mixture.

$$\rho_{COSMO} = (x_{4-Me})\left(\rho_{COSMO,4-Me}\right) + (1 - x_{4-Me})\left(\rho_{COSMO,5-Me}\right) \quad \textbf{(2)}$$

Using the parameters fitted to experimental data (Table 4), linearly interpolated values for densities of for $[RC_1^{(4/5)}mim][Tf_2N]$ and $[RC_2^{(2)}C_1^{(4/5)}mim][Tf_2N]$ at 298.15 are compared against the COSMOTherm calculations (Figure 9). Linearly interpolated values at 298.15 K for $[RC_1^{(2)}mim][Tf_2N]$ and COSMOTherm calculations are also included in this plot.

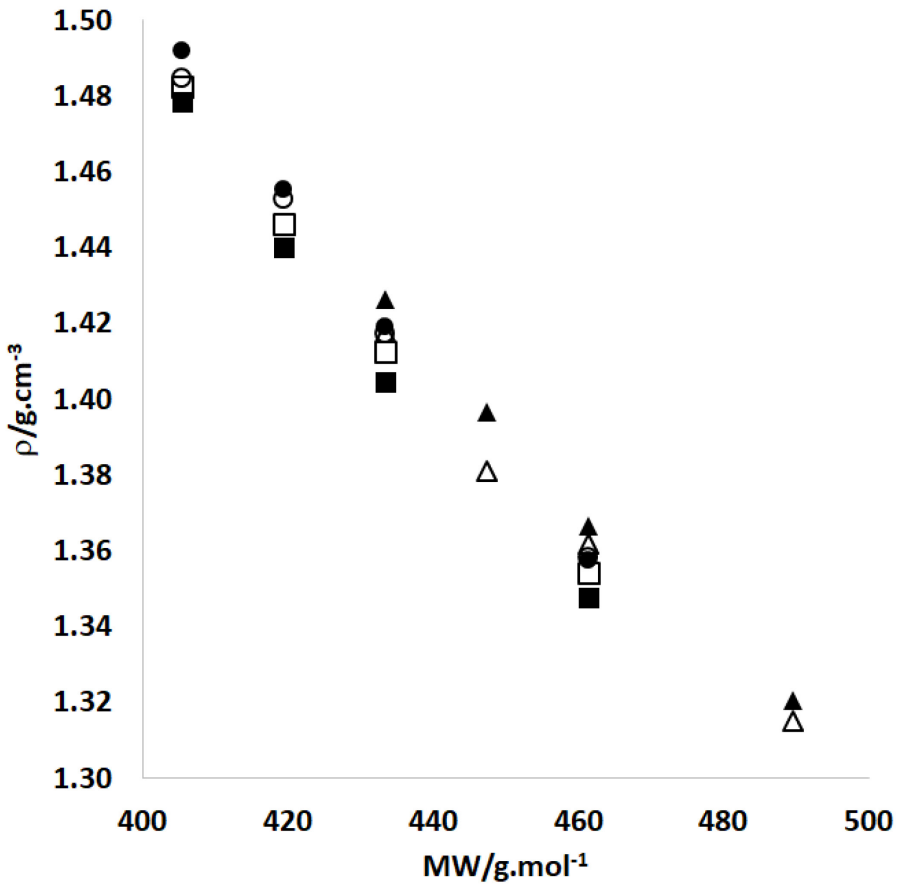

Figure 9: Comparison of experimental (filled) and COSMOTherm calculated (hollow) density relative to molecular weight for: ● = $[RC_1^{(2)}mim][Tf_2N]$; □ ■ = $[RC_1^{(4/5)}mim][Tf_2N]$; ▲△ $[RC_2^{(2)}C_1^{(4/5)}mim][Tf_2N]$.

Figure 9 shows that COSMOTherm calculates the density of all groups of ILs experimentally measured in this work to within ~0.60 % or less, except for $[C_3C_2^{(2)}C_1^{(4/5)}mim][Tf_2N]$ which shows a ~1.10 % difference between the experimental and calculated value. Densities for $[RC_1^{(2)}mim][Tf_2N]$ and $[RC_2^{(2)}C_1^{(4/5)}mim][Tf_2N]$ ILs are slightly underestimated, while those for $[RC_1^{(4/5)}mim][Tf_2N]$ ILs are slightly overestimated. The best agreement between experimental and calculated values is observed for the $[RC_1^{(2)}mim][Tf_2N]$ ILs. As mentioned in Section 3, only the straight-chain conformers were considered in the COSMOTherm calculations, so it may be that the inclusion of other conformers for $[RC_1^{(4/5)}mim][Tf_2N]$ and $[RC_2^{(2)}C_1^{(4/5)}mim][Tf_2N]$ ILs could improve the accuracy of the calculated densities for these groups of ILs. The slope of the relationship between density and the molecular weight of the ILs within groups is well-modeled using by COSMOTherm.

Given the ~1 % or less difference in experimental density and the COSMOTherm calculation, FFV in these ILs as well as for $[RC_2^{(2)}mim][Tf_2N]$ and $[RC_{i\text{-}3}^{(2)}mim][Tf_2N]$ ILs (cf. Figure 1) was calculated using Eqn 1. FFV for $[Rmim][Tf_2N]$ ILs from our prior work were also included to compare how the distribution of alkyl groups about the imidazolium cation affects FFV. Figure 5 presents a plot of FFV relative to IL MW for these 8 groups of ILs. With the exception of $[Rmim][Tf_2N]$ ILs, values for all other ILs are only shown for R = C_2, C_3, C_4 and C_6 in Figure 10.

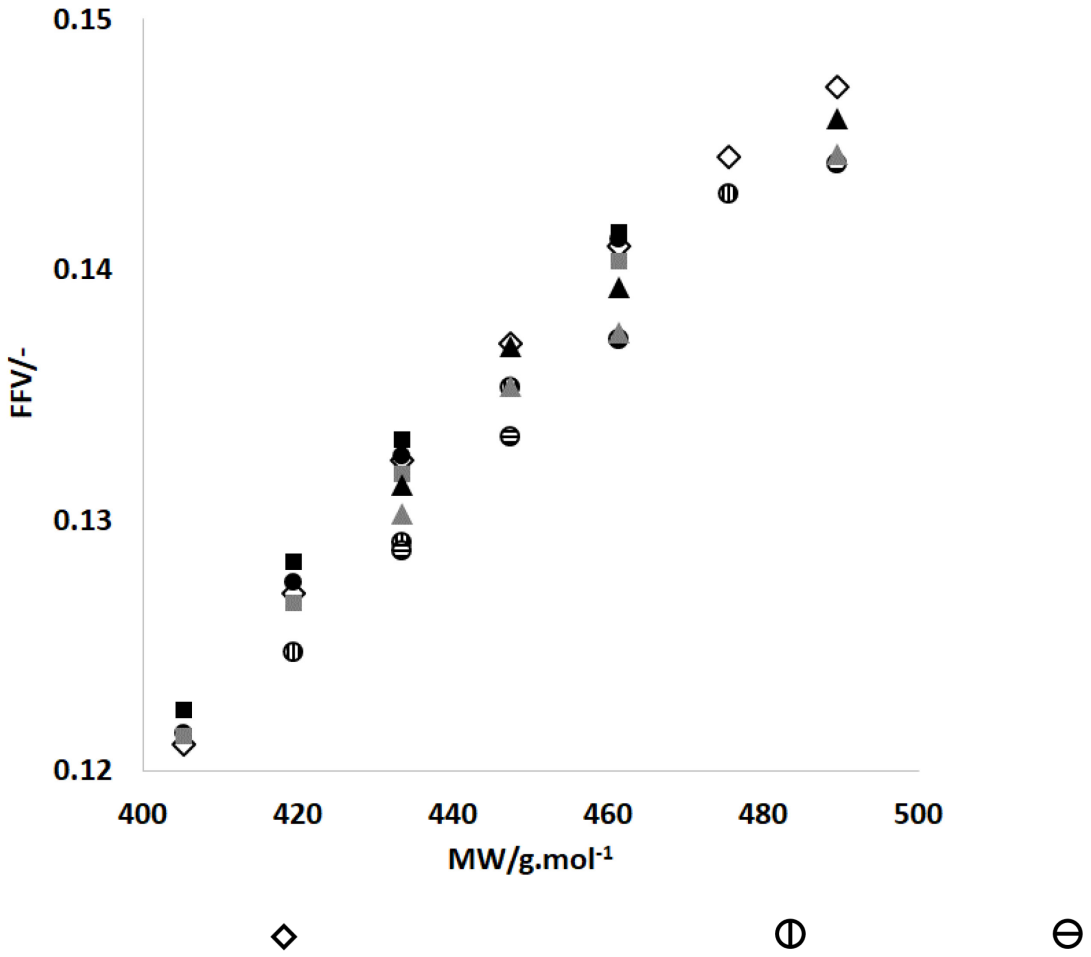

Figure 10 illustrates that for all cation substitution patterns, FFV increases with MW, or increasing length of substituent at the N(1) position. This is fully consistent with results from our prior work. However, within groups of isomers, especially at 443.39 g.mol^{-1}, there is a distinct difference in FFV based on how the alkyl groups are distributed around the imidazolium ring. For all relevant examples, the [RC$_1^{(4)}$mim] and [RC$_1^{(2)}$mim] exhibit the greatest FFV, followed by [Rmim] and [RC$_1^{(5)}$mim] cations, while the [RC$_{i\text{-}3}^{(2)}$mim] cation has the smallest FFV, with [RC$_2^{(2)}$mim] cations only marginally greater. These trends indicate that functionalization of the C(2) and/or C(4) positions of the imidazolium ring with a methyl group can modestly increase FFV relative to the [Rmim] baseline, perhaps up to 1-2 %. Correspondingly, introducing ethyl or isopropyl groups at the C(2) position can reduce FFV relative to the [Rmim] baseline by up to 3 %. While these changes in FFV associated with isomer connectivity are small in their magnitude, small changes in FFV may have larger influences on properties such as gas diffusivity,[64] which would be of interest to imidazolium-based poly(IL) and ionene gas separation membranes formed from ILs or around imidazolium cations.

5. CONCLUSIONS

The densities $[RC_2^{(4/5)}mim][Tf_2N]$, $[RC_1^{(4/5)}mim][Tf_2N]$ and $[RC_2^{(2)}C_1^{(4/5)}mim][Tf_2N]$ ILs were measured over the range of (293.15 to 373.15) K. Densities were observed to decrease with increasing temperature, and increase as substituents were introduced to the C(2), C(4) and/or C(5) positions. COSMOTherm calculations indicate that for $[RC_1^{(4/5)}mim][Tf_2N]$ and $[RC_2^{(2)}C_1^{(4/5)}mim][Tf_2N]$ ILs, the 5-methyl isomers are denser than the 4-methyl isomers. COSMOTherm calculations also indicate that within groups of constitutional isomers, FFV is largest for $[RC_1^{(4)}mim]$ cations and smallest for $[RC_{i\text{-}3}^{(2)}mim]$ cations relative to [Rmim] cations. To the best of our knowledge, this is the first literature report of any density measurements or application of COSMOTherm as a predictive tool for the properties $[RC_1^{(4/5)}mim][Tf_2N]$ or $[RC_2^{(2)}C_1^{(4/5)}mim][Tf_2N]$ ILs. The study of tri-, tetra- and penta-functionalized imidazolium cations is certainly very underexplored compared to relatively simple [Rmim][X] ILs and there is ample opportunity for fundamental studies on structure-property relationships on these salts as well as their use as building blocks for more sophisticated poly(IL) and ionene-based materials.[65]

ACKNOWLEDGMENT

Partial support from the National Science Foundation (CBET-1604511) is gratefully acknowledged. Acknowledgment is made to the donors of the American Chemical Society – Petroleum Research Fund for partial support of this work. The authors thank Dr. Kenneth A. Belmore of the Dept. of Chemistry at the University of Alabama for his assistance in obtaining ^1H NMR spectra.

SUPPORTING INFORMATION AVAILABLE

The Supporting Information is available free of charge on the ACS Publications website at DOI: 10.1021/acs.jced.XXXXXX:

Details on the structure of the cations and anions and their names, abbreviations, and CAS numbers. All calculated data from COSMOTherm. ^1H NMR spectra for ILs 1-12.

REFERENCES

1. Rogers, R. D.; Seddon, K. R. Ionic Liquids--Solvents of the Future? *Science* **2003,** *302*, 792-793.
2. Zaitsau, D. H.; Varfolomeev, M. A.; Verevkin, S. P.; Stanton, A. D.; Hindman, M. S.; Bara, J. E. Structure-property relationships in ionic liquids: Influence of branched and cyclic groups on vaporization enthalpies of imidazolium-based ILs. *J. Chem. Thermodyn.* **2016,** *93*, 151-156.
3. Tang, S.; Baker, G. A.; Zhao, H. Ether- and alcohol-functionalized task-specific ionic liquids: attractive properties and applications. *Chem. Soc. Rev.* **2012,** *41*, 4030-4066.
4. Camper, D.; Bara, J. E.; Gin, D. L.; Noble, R. D. Room-Temperature Ionic Liquid-Amine Solutions: Tunable Solvents for Efficient and Reversible Capture Of CO_2. *Ind. Eng. Chem. Res.* **2008,** *47*, 8496-8498.
5. Bara, J. E.; Gabriel, C. J.; Lessmann, S.; Carlisle, T. K.; Finotello, A.; Gin, D. L.; Noble, R. D. Enhanced CO_2 separation selectivity in oligo(ethylene glycol) functionalized room-temperature ionic liquids. *Ind. Eng. Chem. Res.* **2007,** *46*, 5380-5386.
6. Horne, W. J.; Shannon, M. S.; Bara, J. E. Correlating fractional free volume to CO_2 selectivity in [Rmim][Tf_2N] ionic liquids. *J. Chem. Thermodyn.* **2014,** *77*, 190-196.
7. Smith, G. D.; Borodin, O.; Li, L. Y.; Kim, H.; Liu, Q.; Bara, J. E.; Gin, D. L.; Noble, R. D. A comparison of ether- and alkyl-derivatized imidazolium-based room-temperature ionic liquids: a molecular dynamics simulation study. *Phys. Chem. Chem. Phys.* **2008,** *10*, 6301-6312.
8. Triolo, A.; Russina, O.; Caminiti, R.; Shirota, H.; Lee, H. Y.; Santos, C. S.; Murthy, N. S.; Castner, E. W., Jr. Comparing intermediate range order for alkyl- vs. ether-substituted cations in ionic liquids. *Chem. Commun.* **2012,** *48*, 4959-4961.
9. Zaitsau, D. H.; Yermalayeu, A. V.; Verevkin, S. P.; Bara, J. E.; Wallace, D. A. Structure-property relationships in ionic liquids: Chain length dependence of the vaporization enthalpies of imidazolium-based ionic liquids with fluorinated substituents. *Thermochim. Acta* **2015,** *622*, 38-43.
10. Smith, G. D.; Borodin, O.; Magda, J. J.; Boyd, R. H.; Wang, Y. S.; Bara, J. E.; Miller, S.; Gin, D. L.; Noble, R. D. A comparison of fluoroalkyl-derivatized imidazolium:TFSI and alkyl-derivatized imidazolium:TFSI ionic liquids: a molecular dynamics simulation study. *Phys. Chem. Chem. Phys.* **2010,** *12*, 7064-7076.
11. Bara, J. E.; Gabriel, C. J.; Carlisle, T. K.; Camper, D. E.; Finotello, A.; Gin, D. L.; Noble, R. D. Gas separations in fluoroalkyl-functionalized room-temperature ionic liquids using supported liquid membranes. *Chem. Eng. J.* **2009,** *147*, 43-50.
12. Bara, J. E.; Carlisle, T. K.; Gabriel, C. J.; Camper, D.; Finotello, A.; Gin, D. L.; Noble, R. D. Guide to CO_2 Separations in Imidazolium-Based Room-Temperature Ionic Liquids. *Ind. Eng. Chem. Res.* **2009,** *48*, 2739-2751.
13. Mahurin, S. M.; Dai, T.; Yeary, J. S.; Luo, H.; Dai, S. Benzyl-Functionalized Room Temperature Ionic Liquids for CO_2/N_2 Separation. *Ind. Eng. Chem. Res.* **2011,** 50, 14061-14069.
14. Shirota, H.; Wishart, J. F.; Castner, E. W. Intermolecular interactions and dynamics of room temperature ionic liquids that have silyl- and siloxy-substituted imidazolium cations. *J. Phys. Chem. B* **2007,** *111*, 4819-4829.
15. Seddon, K. R.; Stark, A.; Torres, M. J. Viscosity and density of 1-alkyl-3-methylimidazolium ionic liquids. In *Clean Solvents - Alternative Media for Chemical Reactions and Processing*, Abraham, M. A.; Moens, L., Eds. **2002**; Vol. 819, pp 34-49.
16. Holbrey, J. D.; Rogers, R. D.; Mantz, R. A.; Trulove, P. C.; Cocalia, V. A.; Visser, A. E.; Anderson, J. L.; Anthony, J. L.; Brennecke, J. F.; Maginn, E. J.; Welton, T., Physicochemical Properties. In *Ionic Liquids in Synthesis*, 2nd ed.; Wasserscheid, P.; Welton, T., Eds. Wiley-VCH: Weinheim, Germany, **2008**.
17. Aparicio, S.; Atilhan, M.; Karadas, F. Thermophysical Properties of Pure Ionic Liquids: Review of Present Situation. *Ind. Eng. Chem. Res.* **2010,** *49*, 9580-9595.

18. Ye, C. F.; Shreeve, J. M. Rapid and accurate estimation of densities of room-temperature ionic liquids and salts. *J. Phys. Chem. A* **2007,** *111*, 1456-1461.
19. Gardas, R. L.; Coutinho, J. A. P. Extension of the Ye and Shreeve group contribution method for density estimation of ionic liquids in a wide range of temperatures and pressures. *Fluid Phase Equilibr.* **2008,** *263*, 26-32.
20. Bara, J. E.; Camper, D. E.; Gin, D. L.; Noble, R. D. Room-Temperature Ionic Liquids and Composite Materials: Platform Technologies for CO_2 Capture. *Acc. Chem. Res.* **2010,** *43*, 152-159.
21. Karadas, F.; Atilhan, M.; Aparicio, S. Review on the Use of Ionic Liquids (ILs) as Alternative Fluids for CO_2 Capture and Natural Gas Sweetening. *Energy Fuel.* **2010,** *24*, 5817-5828.
22. Ramdin, M.; de Loos, T. W.; Vlugt, T. J. H. State-of-the-Art of CO_2 Capture with Ionic Liquids. *Ind. Eng. Chem. Res.* **2012,** *51*, 8149-8177.
23. Zeng, S.; Zhang, X.; Bai, L.; Zhang, X.; Wang, H.; Wang, J.; Bao, D.; Li, M.; Liu, X.; Zhang, S. Ionic-Liquid-Based CO2 Capture Systems: Structure, Interaction and Process. *Chem. Rev.* **2017,** *117*, 9625-9673.
24. Shiflett, M. B.; Maginn, E. J. The solubility of gases in ionic liquids. *AIChE J.* **2017,** *63*, 4722-4737.
25. Maginn, E. J. Atomistic Simulation of the Thermodynamic and Transport Properties of Ionic Liquids. *Acc. Chem. Res.* **2007,** *40*, 1200-1207.
26. Bara, J. E. Considering the Basis of Accounting for CO_2 Mole Fractions in Ionic Liquids and Its Influence on the Interpretation of Solution Nonideality. *Ind. Eng. Chem. Res.* **2013,** *52*, 3522-3529.
27. Carvalho, P. J.; Kurnia, K. A.; Coutinho, J. A. P. Dispelling some myths about the CO_2 solubility in ionic liquids. *Phys. Chem. Chem. Phys.* **2016,** 18, 14757-14771.
28. Carvalho, P. J.; Coutinho, J. o. A. P. On the Nonideality of CO_2 Solutions in Ionic Liquids and Other Low Volatile Solvents. *J. Phys. Chem. Lett.* **2010,** *1*, 774-780.
29. Shannon, M. S.; Tedstone, J. M.; Danielsen, S. P. O.; Hindman, M. S.; Irvin, A. C.; Bara, J. E. Free Volume as the Basis of Gas Solubility and Selectivity in Imidazolium-Based Ionic Liquids. *Ind. Eng. Chem. Res.* **2012,** *51*, 5565-5576.
30. Fumino, K.; Peppel, T.; Geppert-Rybczynska, M.; Zaitsau, D. H.; Lehmann, J. K.; Verevkin, S. P.; Kockerling, M.; Ludwig, R. The influence of hydrogen bonding on the physical properties of ionic liquids. *Phys. Chem. Chem. Phys.* **2011,** *13*, 14064-14075.
31. Peppel, T.; Roth, C.; Fumino, K.; Paschek, D.; Köckerling, M.; Ludwig, R. The Influence of Hydrogen-Bond Defects on the Properties of Ionic Liquids. *Angew. Chem. Int. Ed.* **2011,** *50*, 6661-6665.
32. Fumino, K.; Wulf, A.; Ludwig, R. The potential role of hydrogen bonding in aprotic and protic ionic liquids. *Phys. Chem. Chem. Phys.* **2009,** *11*, 8790-8794.
33. Bara, J. E.; Shannon, M. S. Beyond 1,3-difunctionalized imidazolium cations. *Nanomater. Energy* **2012,** 1, 237-242.
34. Lin, B.; Dong, H.; Li, Y.; Si, Z.; Gu, F.; Yan, F. Alkaline Stable C2-Substituted Imidazolium-Based Anion-Exchange Membranes. *Chem. Mater.* **2013,** 25, 1858-1867.
35. Awad, W. H.; Gilman, J. W.; Nyden, M.; Harris Jr, R. H.; Sutto, T. E.; Callahan, J.; Trulove, P. C.; DeLong, H. C.; Fox, D. M. Thermal degradation studies of alkyl-imidazolium salts and their application in nanocomposites. *Thermochim. Acta* **2004,** *409*, 3-11.
36. Bonhôte, P.; Dias, A.-P.; Papageorgiou, N.; Kalyanasundaram, K.; Grätzel, M. Hydrophobic, Highly Conductive Ambient-Temperature Molten Salts. *Inorg. Chem.* **1996,** *35*, 1168-1178.
37. Hayashi, K.; Nemoto, Y.; Akuto, K.; Sakurai, Y. Alkylated imidazolium salt electrolyte for lithium cells. *J. Power Sources* **2005,** *146*, 689-692.
38. Gabric, B.; Sander, A.; Bubalo, M. C.; Macut, D. Extraction of S- and N-compounds from the mixture of hydrocarbons by ionic liquids as selective solvents. *Sci. World J.* **2013**, 512953.
39. Evjen, S.; Fiksdahl, A. Syntheses of polyalkylated imidazoles. *Synth. Commun.* **2017,** 47*,* 1392-1399.

40. Debus, H. Ueber die Einwirkung des Ammoniaks auf Glyoxal. *Liebigs Ann. Chem.* **1858,** 107, 199-208.
41. Wang, Z. 518. Radziszewski Reaction. In *Comprehensive Organic Name Reactions and Reagents*, John Wiley & Sons, Inc.: Hoboken, NJ USA, **2009**; Vol. 3, pp 2293-2297.
42. Radziszewski, B. Ueber die Synthese der Oxalinbasen. *Berichte Dtcsh. Chem. Ges.* **1883,** *16*, 487-494.
43. Radziszewski, B. Ueber einige neue Glyoxaline. *Berichte Dtcsh. Chem. Ges.* **1883,** *16*, 747-749.
44. Radziszewski, B. Ueber die Constitution des Lophins und verwandter Verbindungen. *Berichte Dtcsh. Chem. Ges.* **1882,** *15*, 1493-1496.
45. Hindman, M. S.; Stanton, A. D.; Irvin, A. C.; Wallace, D. A.; Moon, J. D.; Reclusado, K. R.; Liu, H.; Belmore, K. A.; Liang, Q.; Shannon, M. S.; Turner, C. H.; Bara, J. E. Synthesis of 1,2-dialkyl-, 1,4(5)-dialkyl-, and 1,2,4(5)-trialkylimidazoles via a one-pot method. *Ind. Eng. Chem. Res.* **2013,** *52*, 11880-11887.
46. Maton, C.; De Vos, N.; Roman, B. I.; Vanecht, E.; Brooks, N. R.; Binnemans, K.; Schaltin, S.; Fransaer, J.; Stevens, C. V. Continuous Synthesis of Peralkylated Imidazoles and their Transformation into Ionic Liquids with Improved (Electro)Chemical Stabilities. *ChemPhysChem* **2012,** *13*, 3146-3157.
47. Ludwig, R.; Paschek, D. Applying the Inductive Effect for Synthesizing Low-Melting and Low-Viscosity Imidazolium-Based Ionic Liquids. *ChemPhysChem* **2009,** *10*, 516-519.
48. Roth, C.; Peppel, T.; Fumino, K.; Köckerling, M.; Ludwig, R. The Importance of Hydrogen Bonds for the Structure of Ionic Liquids: Single-Crystal X-ray Diffraction and Transmission and Attenuated Total Reflection Spectroscopy in the Terahertz Region. *Angew. Chem. Int. Ed.* **2010,** *49*, 10221-10224.
49. Fredlake, C. P.; Crosthwaite, J. M.; Hert, D. G.; Aki, S. N. V. K.; Brennecke, J. F. Thermophysical Properties of Imidazolium-Based Ionic Liquids. *J. Chem. Eng. Data* **2004,** *49*, 954-964.
50. Katsuta, S.; Shiozawa, Y.; Imai, K.; Kudo, Y.; Takeda, Y. Stability of Ion Pairs of Bis(trifluoromethanesulfonyl)amide-Based Ionic Liquids in Dichloromethane. *J. Chem. Eng. Data* **2010,** *55*, 1588-1593.
51. Ren, R.; Zuo, Y.; Zhou, Q.; Zhang, H.; Zhang, S. Density, Excess Molar Volume and Conductivity of Binary Mixtures of the Ionic Liquid 1,2-Dimethyl-3-hexylimidazolium Bis(trifluoromethylsulfonyl)imide and Dimethyl Carbonate. *J. Chem. Eng. Data* **2011,** *56*, 27-30.
52. Papović, S.; Vraneš, M.; Kordić, B.; Filipović, S.; Bešter-Rogač, M.; Gadžurić, S. Interactions of 1,2,3-trialkylimidazolium-based ionic liquids with γ-butyrolactone. *J. Chem. Thermodyn.* **2016,** *101*, 260-269.
53. Gaciño, F. M.; Regueira, T.; Lugo, L.; Comuñas, M. J. P.; Fernández, J. Influence of Molecular Structure on Densities and Viscosities of Several Ionic Liquids. *J. Chem. Eng. Data* **2011,** *56*, 4984-4999.
54. Shannon, M. S.; Bara, J. E. Properties of Alkylimidazoles as Solvents for CO_2 Capture and Comparisons to Imidazolium-Based Ionic Liquids. *Ind. Eng. Chem. Res.* **2011,** *50*, 8665-8677.
55. Bara, J. E.; Moon, J. D.; Reclusado, K. R.; Whitley, J. W. COSMOTherm as a Tool for Estimating the Thermophysical Properties of Alkylimidazoles as Solvents for CO_2 Separations. *Ind. Eng. Chem. Res.* **2013,** *52*, 5498-5506.
56. Palomar, J.; Gonzalez-Miquel, M.; Polo, A.; Rodriguez, F. Understanding the Physical Absorption of CO_2 in Ionic Liquids Using the COSMO-RS Method. *Ind. Eng. Chem. Res.* **2011,** *50*, 3452-3463.
57. Diedenhofen, M.; Klamt, A. COSMO-RS as a tool for property prediction of IL mixtures-A review. *Fluid Phase Equilibr.* **2010,** *294*, 31-38.
58. Schaefer, A.; Huber, C.; Ahlrichs, R. Fully optimized contracted Gaussian basis sets of triple zeta valence quality for atoms Li to Kr. *J. Chem. Phys.* **1994,** *100*, 5829-35.
59. Becke, A. D. Density-functional exchange-energy approximation with correct asymptotic behavior. *Phys. Rev. A* **1988,** *38*, 3098-3100.
60. Perdew, J. P. Density-functional approximation for the correlation energy of the inhomogeneous electron gas. *Phys. Rev. B* **1986,** *33,* 8822-8824.

61. NIST, Ionic Liquids Database (ILThermo) NIST Standard Reference Database #147. http://ilthermo.boulder.nist.gov/ Accessed 28 November 2017.
62. Widegren, J. A.; Magee, J. W. Density, Viscosity, Speed of Sound, and Electrolytic Conductivity for the Ionic Liquid 1-Hexyl-3-methylimidazolium Bis(trifluoromethylsulfonyl)imide and Its Mixtures with Water. *J. Chem. Eng. Data* **2007,** *52*, 2331-2338.
63. Rocha, M. A. A.; Neves, C. M. S. S.; Freire, M. G.; Russina, O.; Triolo, A.; Coutinho, J. A. P.; Santos, L. M. N. B. F. Alkylimidazolium Based Ionic Liquids: Impact of Cation Symmetry on Their Nanoscale Structural Organization. *J. Phys. Chem. B* **2013,** *117*, 10889-10897.
64. Lee, W. M. Selection of Barrier Materials from Molecular Structure. *Polym. Eng. Sci.* **1980,** *20*, 65-69.
65. Mittenthal, M. S.; Flowers, B. S.; Bara, J. E.; Whitley, J. W.; Spear, S. K.; Roveda, J. D.; Wallace, D. A.; Shannon, M. S.; Holler, R.; Martens, R.; Daly, D. T. Ionic Polyimides: Hybrid Polymer Architectures and Composites with Ionic Liquids for Advanced Gas Separation Membranes. *Ind. Eng. Chem. Res.* **2017,** *56*, 5055-5069.

For Table of Contents Only